Séminaire Lotharingien de Combinatoire **XX** (2026)
Article #YY, 12 pp.

Proceedings of the 38th Conference on Formal Power Series and Algebraic Combinatorics (Seattle)

The periodic multi-layer polynuclear growth: Integrability and applications

Takashi Imamura*[1], Matteo Mucciconi[2], Tomohiro Sasamoto[3], and Travis Scrimshaw†[4]

[1]*Department of Mathematics and Informatics, Chiba University, Japan*
[2]*Department of Mathematics, National University of Singapore, Singapore*
[3]*Department of Physics, Institute of Science Tokyo, Japan*
[4]*Department of Mathematics, Hokkaido University, Japan*

Abstract. We introduce the periodic multi-layer polynuclear growth dynamics, a deterministic evolution of sequences of height function $(h_i(x,t))_{i\in\mathbb{Z}}$, where $x \in \mathbb{R}/\mathbb{Z}$ and $t \in \mathbb{R}$ is the time. This dynamics is integrable: it possesses solitionic behavior, it has a rich set of symmetries and can be reduced, through a projection to the box-ball system (BBS). The inverse scattering map is a generalization of Kerov–Kirillov–Reshetikhin, which linearizes the BBS dynamics. The action of the inverse scattering map on special classes of initial data yields bijective proofs of summation identities for transformed Hall–Littlewood polynomials. These have applications in the description of height distribution of growth processes.

Keywords: Robinson–Schensted–Knuth correspondence, Fomin growth rule, box-ball system, Macdonald polynomials

1 Introduction

Let $\mathbb{T} = \mathbb{R}/\mathbb{Z}$ be the unit interval with periodic boundary conditions. Introduce the set of piecewise constant integer valued functions on $\mathbb{T}$ with finite unit jump discontinuities

$$\mathsf{PW}_{\mathbb{T}} = \{h\colon \mathbb{T} \to \mathbb{Z} : h(x) - h(x_{\pm}) \in \{0,1\}\ \forall x \text{ and } |\{x : h(x) \neq h(x_{\pm})\}| < \infty\}, \quad (1.1)$$

where $h(x_{\pm}) = \lim_{\varepsilon\downarrow 0} h(x \pm \varepsilon)$ and $|A|$ denotes the cardinality of the set A. We refer to functions in $\mathsf{PW}_{\mathbb{T}}$ as height functions. A point $x \in \mathbb{T}$ is an up-jump (resp. down-jump) for $h \in \mathsf{PW}_{\mathbb{T}}$ if $h(x) - h(x_-) > 0$ (resp. if $h(x) - h(x_+) > 0$) and it is a point of continuity otherwise. We introduce the set of ordered sequences of height functions with finitely many discontinuities

$$\mathcal{S} = \{(h_i)_{i\in\mathbb{Z}} \subset \mathsf{PW}_{\mathbb{T}} : h_i(x) > h_{i+1}(x)\ \forall i, x \text{ and } |\{(i,x) : h_i(x) \neq h_i(x_{\pm})\}| < \infty\}. \quad (1.2)$$

*imamura@math.s.chiba-u.ac.jp. Takashi Imamura was partially supported by JSPS Grant-in-Aid 22H01143, 24K06773.

†Travis Scrimshaw was partially supported by JSPS Grant-in-Aid 23K12983.

The set $\mathcal{S}$ will be the space of states for the *periodic multi-layer polynuclear growth* (*periodic PNG*), a deterministic dynamics $\boldsymbol{h}(t) = (h_i(t))_{i\in\mathbb{Z}}$ that we introduce next. In the periodic PNG, functions h_i evolve following two rules:

1. **(Lateral propagation)** For each $i \in \mathbb{Z}$ the up-jumps of h_i move with unit speed to their left while the down-jumps move with unit speed to their right.

2. **(Layer-to-layer propagation)** If a down-jump and an up-jump of h_i collide at a point x at time t, they annihilate, triggering a nucleation at level $i+1$ and $h_{i+1}(y,t) = h_{i+1}(y,t_-) + \mathbf{1}_{y=x}$.

We denote by $\{\phi_t\}_{t\in\mathbb{R}}$ the periodic PNG flow and given $h \in \mathcal{S}$ we denote by $\boldsymbol{h}(t) = \phi_t[h]$ the collection of lines following the periodic PNG dynamics with initial data $\boldsymbol{h}(0) = h \in \mathcal{S}$. It could happen that along the dynamics, for some time t, $\boldsymbol{h}(t) \notin \mathcal{S}$, if a nucleation takes place right on top of a discontinuity point. To make the discussion lighter, we rule out such situations defining the set $\mathring{\mathcal{S}}$ of configurations h such that the evolution $\phi_t[h]$ remains on $\mathcal{S}$ for all times $t \in \mathbb{R}$

$$\mathring{\mathcal{S}} = \{h \in \mathcal{S} : \phi_t[h] \in \mathcal{S} \ \forall t \in \mathbb{R}\}. \tag{1.3}$$

Remark 1. The periodic PNG generalizes the multi-layer PNG introduced in [15]. To realize the latter, informally, one needs to take $h_0(x,0) \gg 0$ and set the law of $h_{-k}(x,0)$, for $k \geq 0$ as non-intersecting random walk bridges with exponential waiting times. Such law is stationary in the sense that $h_{-k}(x,t)$ will remain non-intersecting random walk bridges. Moreover the nucleation induced on the layer h_1 have space-time Poisson rate. A large scaling of the cylinder's diameter recovers the full space PNG.

A run of the periodic PNG reveals that it possesses solitonic behavior, demonstrated by the conservation of wave-like structures upon collisions: see Figure 1. These conservation laws are consequence of the large number of symmetries enjoyed by the periodic PNG and that we describe in this note. Studying such symmetries we connect the periodic PNG and the box-ball system, as explained in Section 3. The main result we present in Theorem 2 is an explicit linearization scheme for the periodic PNG and the proof is outlined in Section 3.2. For its statement we introduce several preliminary notions.

For an integer partition μ we define $\mathrm{HST}(\mu)$ to be the set of *horizontally standard tableaux*, which are filling of the Young diagram of μ with labels in $\{1,\dots,|\mu|\}$ without repetitions and which are increasing row-wise. We also define $\mathcal{K}(\mu) = \{\kappa = (\kappa_1,\dots,\kappa_{\ell(\mu)}) \in \mathbb{Z}^{\ell(\mu)} : \kappa_i \geq \kappa_{i+1} \text{ if } \mu_i = \mu_{i+1}\}$. Also define the set $\mathbb{S}$ of weakly decreasing integer valued bi-infinite sequences $\mathbb{S} = \{\nu = (\nu_i)_{i\in\mathbb{Z}} \subset \mathbb{Z} : \nu_i \geq \nu_{i+1} \ \forall\, i\}$. Finally we denote by $\mathcal{D}_n = \{\boldsymbol{x} = (x_1,\dots,x_n) \in (-1/2,0]^n : x_1 < \cdots < x_n\}$.

Theorem 2. *There exists an explicit bijection*

$$h \in \mathring{\mathcal{S}} \xleftrightarrow{\ \psi\ } (H_1, H_2, \kappa, \nu, \boldsymbol{x}, \boldsymbol{x}') \in \bigsqcup_{n\geq 0} \bigsqcup_{\mu\vdash n} \Big(\mathrm{HST}(\mu)^2 \times \mathcal{K}(\mu)\Big) \times \mathbb{S} \times \mathcal{D}_n^2$$

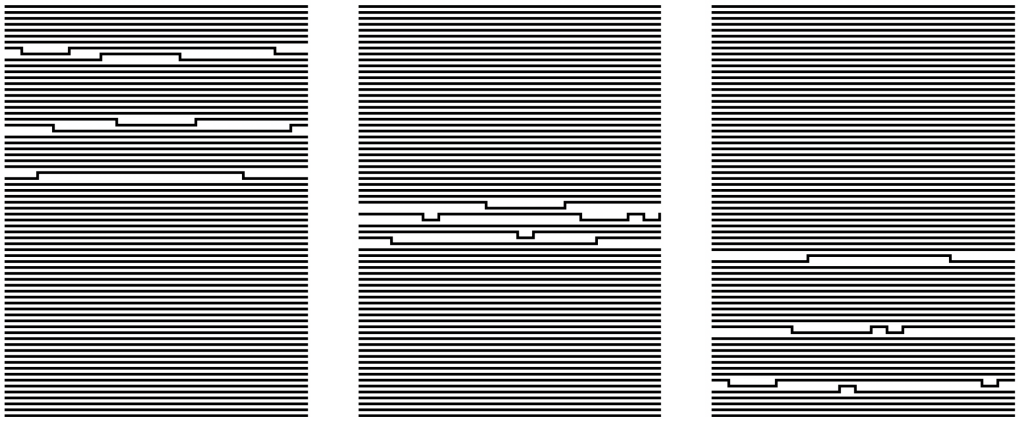

Figure 1: Snapshots of a periodic multi-layer PNG dynamics $\boldsymbol{h}(t_1), \boldsymbol{h}(t_2), \boldsymbol{h}(t_3)$ at times $t_1 < t_2 < t_3$. In the first and third panel the configurations consist of three wave-like formations respectively of 1, 2 and 3 islands (i.e. pairs of up-jumps and down-jumps) well spaced from each other. In the central panel the wave-like formations are mixed.

such that, for all $\tau \in \mathbb{Z}$, $\psi(\phi_\tau[h]) = (H_1, H_2; \kappa + \tau\,\mu, \nu, \boldsymbol{x}, \boldsymbol{x}')$.

2 Symmetries of the periodic PNG

We use the notion of Young tableaux of skew shape λ/ρ. For us λ, ρ will always be signatures of the same length ℓ, i.e. non-increasing sequences of ℓ integers satisfying $\rho_i \leq \lambda_i$, for all i. In this case in this case we write $|\lambda/\rho| = \sum_i \lambda_i - \rho_i$. A skew signature λ/ρ can be seen as its Young diagram, the set of cells (k, j) such that $\rho_j \leq k \leq \lambda_j$. A semi-standard Young tableau P of shape λ/ρ, is a filling of cells of λ/ρ which is non-decreasing row-wise and strictly increasing column-wise. Such tableaux is standard if the filling includes all numbers $\{1, \ldots, |\lambda/\rho|\}$. The set of standard Young tableaux of shape λ/ρ is denoted by $\mathrm{ST}(\lambda/\rho)$.

2.1 Robinson–Schensted (RS) dynamics

Introduce the cylinder $\mathcal{C} = \mathbb{T} \times \mathbb{R}$, viewed as a set of space-time coordinates. The periodic PNG dynamics is isotropic and as a result it commutes with space time translations. Moreover, for any $i \in \mathbb{Z}$, nucleations at the i-th layer are independent on the value of h_i. These elementary observations imply the symmetries reported next.

Lemma 3. *Fix* $(\xi, \sigma) \in \mathcal{C}$ *and* $\nu \in \mathbb{S}$. *Define the space shift* $\theta_\xi[f](x) = f(x + \xi)$ *and the maps*

$$\mathcal{T}_{(\xi,\sigma)} \colon h \to \phi_\sigma \circ \theta_\xi[h] \qquad \mathfrak{S}_\nu \colon h \to h + \nu = (h_i(\cdot) + \nu_i)_{i \in \mathbb{Z}}. \tag{2.1}$$

Then $\mathcal{T}_{(\xi,\sigma)}, \mathfrak{S}_\nu$ commute with each other and with the periodic PNG flow, i.e. $\phi_t\left[\mathcal{T}_{(\xi,\sigma)}(h)\right] = \mathcal{T}_{(\xi,\sigma)}\left(\phi_t[h]\right)$ and $\phi_t[\mathfrak{S}_\nu(h)] = \mathfrak{S}_\nu\left(\phi_t[h]\right)$. We refer to the latter as the shift symmetry.

For any $n \in \mathbb{N}$, define $\mathring{\mathcal{S}}_n$ as the set of sequences of height functions in $\mathring{\mathcal{S}}$ with exactly n-up jumps and n-down jumps. We also define the set $\mathcal{P}_n = \{A \subset \mathcal{C} : |A| = n\}$ of n-tuples of distinct points on $\mathcal{C}$ and the set $\mathring{\mathcal{P}}_n$ of n-tuples $\{p_1, \dots, p_n\} \in \mathcal{P}_n$ such that $p_i - p_j \notin (\pm 1, 1)\mathbb{R}$, $\forall\, 1 \le i \ne j \le n$. The following theorem gives a recipe to encode line ensembles in $\mathring{\mathcal{S}}_n$ in terms of n space-time coordinates and a monotonic list of integers.

Theorem 4. *We have an explicit bijection $h \in \mathring{\mathcal{S}}_n \overset{\Upsilon}{\longleftrightarrow} (\boldsymbol{p}, \nu) \in \mathring{\mathcal{P}}_n \times \mathbb{S}$.*

Proof. Let $h \in \mathring{\mathcal{S}}_n$ be a sequence of height functions and let $\boldsymbol{h}(t) = \phi_t[h]$. Define $\nu = (\nu_i)_{i\in\mathbb{Z}}$ setting $\nu_i = \lim_{t\to-\infty} \boldsymbol{h}_i(t) + i - 1$. Then, we set, $\boldsymbol{p} = \{(x_1, t_1), \dots, (x_n, t_n)\} \subset \mathcal{C}$ as the space-time points where nucleations occur at layer $i = 1$; i.e. $h_1(y, t_k) = h_1(y, (t_k)_-) + \mathbf{1}_{y=x_k}$, for $k = 1, \dots, n$. See Figure 3 (first and second panel) for an example. □

Drawing on $\mathcal{C}$ the space-time trajectories of up-jumps and down-jumps with colors corresponding to layers one realizes a periodic shadow lines construction, as in Figure 3 (second and third panel). The following theorem is a variant of the Robinson–Schensted correspondence introduced in [16].

Theorem 5. *We have an explicit injection*

$$h \in \mathring{\mathcal{S}}_n \xrightarrow{\Psi} (P, Q, \nu, \boldsymbol{x}, \boldsymbol{x}') \in \bigsqcup_{|\lambda/\rho|=n} \mathrm{ST}(\lambda/\rho)^2 \times \mathbb{S} \times \mathcal{D}_n^2.$$

Moreover, data $\nu, \boldsymbol{x}, \boldsymbol{x}'$ are invariant under periodic PNG and we call $\widetilde{\Psi}(h) = (P, Q)$.

Proof. Let $h \in \mathring{\mathcal{S}}_n$ and let $\tilde{h} = h - \nu$, where ν is the sequence determined in Theorem 4. Let $\boldsymbol{h}(t) = \phi_t[\tilde{h}]$ be the corresponding periodic PNG evolution which has the property that $\lim_{t\to-\infty} \boldsymbol{h}_i(t) = -i + 1$. Given these asymptotic conditions, the entire evolution $\boldsymbol{h}(t)$ is determined by two n-tuples of pairs $(x_i, c_i)_{i=1,\dots,n}$ and $(x'_i, c'_i)_{i=1,\dots,n}$ with $\boldsymbol{x} = (x_i)_{i=1,\dots,n}, \boldsymbol{x}' = (x'_i)_{i=1,\dots,n} \in \mathcal{D}_n$ and $\boldsymbol{c} = (c_i)_{i=1,\dots,n}, \boldsymbol{c}' = (c'_i)_{i=1,\dots,n} \in \mathbb{Z}^n$ such that $\boldsymbol{c}, \boldsymbol{c}'$ are permutations of each other. A pair (x_i, c_i) (resp. (x'_i, c'_i)) records the presence of an up-jump at layer c_i at space-time (x_i, x_i) (resp. a down-jump at layer c'_i at space-time $(-x'_i, x'_i)$). From the sequence $(p_i, c_i)_{i=1,\dots,n}$, we construct a Young tableau by placing i-labels at cell $(c_i, \boldsymbol{h}_{c_i}(x_i, x_i) + c_i - 1)$. Similarly we construct the Q tableau from the sequence $(x'_i, c'_i)_{i=1,\dots,n}$ by placing i-labels at cell $(c'_i, \boldsymbol{h}_{c'_i}(-x'_i, x_i) + c'_i - 1)$. The example

below constructs the tableaux corresponding to Figure 3 (first three panels).

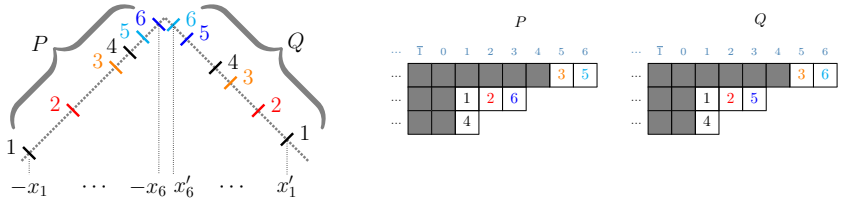

□

Remark 6. We can upgrade the map Ψ to a bijection specifying the set of pairs of tableaux in the image. These pairs of tableaux are minimal in the sense that removing from both of them the same row of empty cells breaks the semi-standard propery.

It is interesting to examine the image of the projection $\widetilde{\Psi}$ at different times of an evolution $\boldsymbol{h}(t)$. This defines a discrete time evolution on the set of pairs of standard Young tableaux $(P_\tau, Q_\tau) = \widetilde{\Psi}(\boldsymbol{h}(\tau))$, for $\tau \in \mathbb{Z}$ that we call *skew RS dynamics*; see Figure 2 (left panel) for an example. An alternative and explicit definition of the skew RS dynamics is given in terms of Schensted's column insertion algorithm. The advantage of the skew RS dynamics is that its symmetries have a clean combinatorial description.

Theorem 7. *There exists a projection* $h \in \mathring{\mathcal{S}}_n \xrightarrow{\Phi} (H_1, H_2) \in \bigsqcup_{|\mu|=n} \mathrm{HST}(\mu)^2$.

Proof. Consider the sequence $(P_\tau, Q_\tau) = \widetilde{\Psi}(\boldsymbol{h}(\tau))$. The rows of tableau H_1 (resp. H_2) are those of the tableau P_τ (resp. Q_τ) for $\tau \to \infty$. In the example of Figure 2, we have

$$H_1 = \begin{array}{|c|c|c|}\hline 2&3&5\\\hline 1&6\\\cline{1-2}4\\\cline{1-1}\end{array}\,, \quad H_2 = \begin{array}{|c|c|c|}\hline 2&3&6\\\hline 1&5\\\cline{1-2}4\\\cline{1-1}\end{array}\,. \tag{2.2}$$

□

2.2 Crystal symmetries of the periodic PNG

On the set of Young tableaux we define the action of Kashiwara operators denoted by $\widetilde{e}_i, \widetilde{f}_i$ for $i \geq 1$. (See, e.g., [5] for more on crystals.) Given a semi-standard Young tableau P the action of $\widetilde{e}_i$ turns an $(i+1)$-label into an i-label through following algorithm. Prepare a word $\boldsymbol{w} = w_1 \cdots w_k$ by reading from bottom-to-top and left-to-right all i and $(i+1)$ labels in the tableau P. Iteratively cancel all consecutive pairs $(i+1), i$ in $\boldsymbol{w}$ until obtaining $\widetilde{\boldsymbol{w}} = i^a(i+1)^b$ for some $a, b \geq 0$. If $b = 0$, set $\widetilde{e}_i(P) = \emptyset$. Otherwise for the cell c in P corresponding to the leftmost $(i+1)$ in $\widetilde{\boldsymbol{w}}$, define $\widetilde{e}_i(P)$ by replacing the $(i+1)$

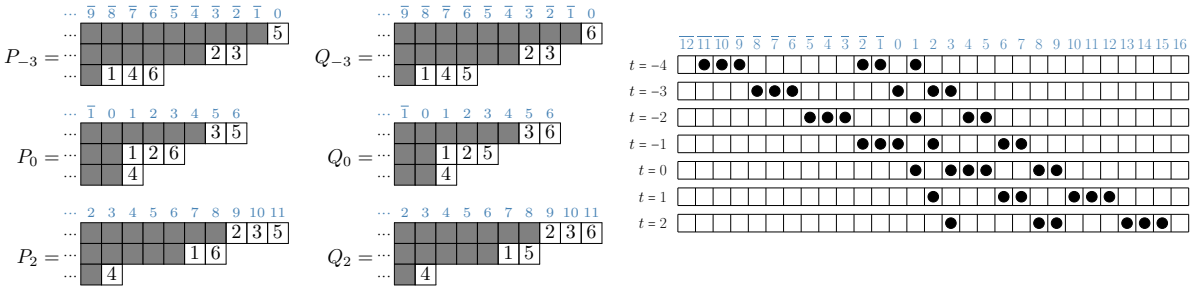

Figure 2: On the left panel an example of the skew RS dynamics with initial data (P_0, Q_0). On the right panel an example of the BBS dynamics.

with an i in c. The operator $\widetilde{f}_i$ is the partial inverse of $\widetilde{e}_i$ and defined analogously by changing the rightmost i in $\widetilde{w}$. We define by $\mathcal{B}_\infty$ the monoid generated by $\widetilde{e}_i$, $\widetilde{f}_i$ for $i \geq 1$.

The bijection Ψ of Theorem 5 allows us to define a large class of transformations on sequences $\mathring{\mathcal{S}}_n$. By Lemma 3, the groups $\mathcal{C}, \mathbb{S}$ (with addition operation) possess natural actions on $\mathring{\mathcal{S}}$. Next, for $b, b' \in \mathcal{B}_\infty$ and[1] $\zeta, \zeta' \in \mathrm{End}(\mathcal{D}_n)$ and $h \in \mathring{\mathcal{S}}$ such that $\Psi(h) = (P, Q, \nu, \boldsymbol{x}, \boldsymbol{x}')$, we define the actions

$$(b, b')(h) := \Psi^{-1}(b(P), b'(Q), \nu, \boldsymbol{x}, \boldsymbol{x}') \qquad (\zeta, \zeta')(h) := \Psi^{-1}(P, Q, \nu, \zeta(\boldsymbol{x}), \zeta'(\boldsymbol{x}')). \tag{2.3}$$

Let G_n be the monoid generated by the action of $\mathcal{C}, \mathbb{S}, \mathcal{B}_\infty^2, \mathrm{End}(\mathcal{D}_n)^2$ on $\mathring{\mathcal{S}}$ by (2.1), (2.3).

Theorem 8. *Let $g \in G_n$ and $h \in \mathring{\mathcal{S}}_n$ such that $g(h) \in \mathring{\mathcal{S}}_n$ exists. Then $\phi_t[g(h)] = g(\phi_t[h])$.*

Remark 9. The action of G_n on pairs $(P, Q) = \widetilde{\Psi}(h)$ (resp. $(H_1, H_2) = \Phi(h)$ induces on $\bigsqcup_{|\lambda/\rho|=n} \mathrm{ST}(\lambda/\rho)^2$ (resp. $\bigsqcup_{|\mu|=n} \mathrm{HST}(\mu)^2$) two commuting $U_q(\widehat{\mathfrak{sl}}_\infty)$ crystal structures.

3 Linearization of periodic PNG and box-ball system

3.1 The box-ball system

The (single species) *box-ball system* (BBS) [17] with n particles is a discrete deterministic, reversible, dynamics on the set $\mathrm{BBS}_n = \{(\eta_i)_{i\in\mathbb{Z}} \in \{0,1\}^{\mathbb{Z}} : \sum_{i\in\mathbb{Z}} \eta_i = n\}$. Given a configuration $\boldsymbol{\eta}(t) = (\eta_i(t))_{i\in\mathbb{Z}}$, the evolution proceeds in discrete time steps. At each step, the configuration at time $t+1$ is obtained from that at time t by moving the particles one by one, from the leftmost to the right, so that each particle jumps to the nearest available empty site to its right; for an example, see Figure 2 (right panel). We denote by $\{\widetilde{\phi}_\tau\}_{\tau\in\mathbb{Z}}$ the discrete flow of the BBS.

[1] Here, for a set A, we denote by $\mathrm{End}(A)$ the set of functions $f : A \to A$.

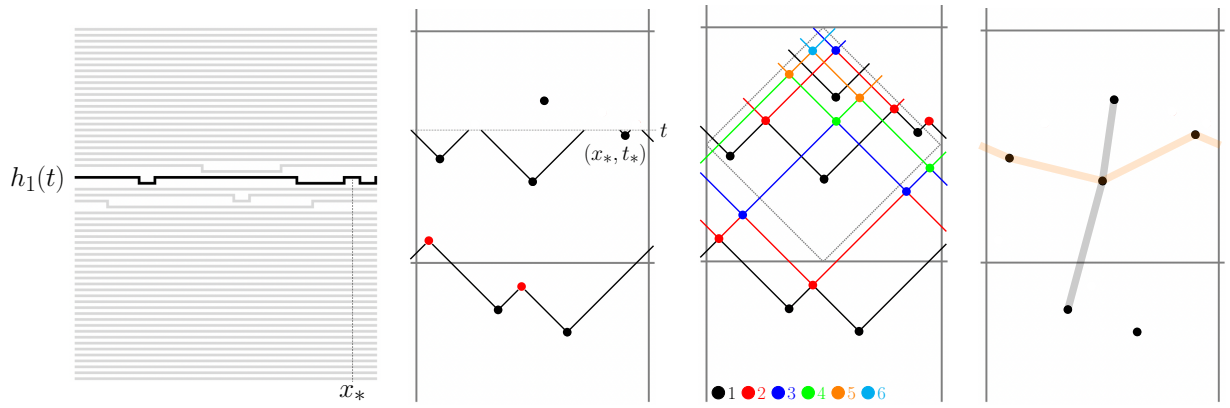

Figure 3: In the first panel a configuration $h \in \mathring{\mathcal{S}}_6$ with h_1 highlighted in black; a nucleation just occurred at layer 1 at x_* and time $t_* < t$. In the second panel black dots are space-time nucleation points over h_1, as in Theorem 4, while black lines are the trajectories of up-jumps and down-jumps of h_1. In the third panel, the periodic shadow line construction, where i colored lines are trajectories of up-jumps and down-jumps at layer h_i. In the fourth panel an up-path in gray and a simple loop in yellow.

The BBS dynamics posses deep mathematical structures and in particular it is integrable; for a review, see [13]. An important construction in the theory of the BBS is the *Kerov-Kirillov-Reschetikhin bijection*. It associates to a BBS configuration $\boldsymbol{\eta}$ a pair (μ, J) where $\mu \vdash n$ is a partition encoding the length of the solitons in $\boldsymbol{\eta}$, while $J \in \mathcal{K}(\mu)$ is a list of integers. The KKR bijection linearizes the BBS dynamics in the sense that, if $KKR(\boldsymbol{\eta}) = (\mu, J)$, then $KKR(\widetilde{\phi}(\boldsymbol{\eta})) = (\mu, J + \mu)$. For example, the image of the $t = 0$ BBS configuration in Figure 2 is $\mu = (3, 2, 1), J = (-3, -1, -1)$.

3.2 From the periodic PNG to the BBS

The vast set of symmetries of the periodic PNG described by Theorem 8 can be used to transform any initial state $h \in \mathring{\mathcal{S}}$ into a simpler state whose dynamics can be fully characterized. Such simpler states are BBS configuration, as described next.

Theorem 10. *There exists an explicit projection* $\mathring{\mathcal{S}}_n \xrightarrow{\pi} \mathsf{BBS}_n$, *which intertwines the PNG and the BBS in the sense that* $\pi(\phi_1[h]) = \widetilde{\phi}_1[\pi(h)]$.

The projection π is an explicit algorithm (described at length in [12]) that combines the action of the crystal operators and isotropic transformations $\mathcal{T}_{(\xi,\sigma)}$ from Lemma 3. In the example of (P_0, Q_0) of Figure 2 one obtains

$$(P_0, Q_0) \longrightarrow (T, T) = \left(\begin{array}{|c|c|c|c|c|c|c|c|c|c|c|} \hline \cdots & 0 & 1 & 2 & 3 & 4 & 5 & 6 & 7 & 8 & 9 \\ \hline \cdots & & & & & & & & & 1 & 1 \\ \hline \cdots & & & & 1 & 1 & 1 & & & & \\ \hline \cdots & & 1 & & & & & & & & \\ \hline \end{array} \;,\; \begin{array}{|c|c|c|c|c|c|c|c|c|c|c|} \hline \cdots & 0 & 1 & 2 & 3 & 4 & 5 & 6 & 7 & 8 & 9 \\ \hline \cdots & & & & & & & & & 1 & 1 \\ \hline \cdots & & & & 1 & 1 & 1 & & & & \\ \hline \cdots & & 1 & & & & & & & & \\ \hline \end{array} \right),$$

where right hand side consists of a pair of identical tableaux having only 1-labels. Setting $\eta_i = 1$ if the i-th column of T posses a 1-labeled cell recovers the BBS configuration.

Sketch of proof of Theorem 2. From a sequence $h \in \mathring{\mathcal{S}}$ we construct data $(H_1, H_2, \kappa, \nu, \boldsymbol{x}, \boldsymbol{x}')$ as follows. The pair $(H_1, H_2) \in \mathrm{HST}(^-)$ is given by Theorem 7, the triple $(\nu, \boldsymbol{x}, \boldsymbol{x}')$ is given by Theorem 5 and finally the sequence κ is given by $\kappa = J - \mu$ where (μ, J) is the image of $\pi(h)$ under the KKR bijection, where π is the projection of Theorem 10. For example, for the state h from Figure 3, we have $\psi(h) = (H_1, H_2, \kappa, \nu, \boldsymbol{x}, \boldsymbol{x}')$ with H_1, H_2 as in (2.2), $\kappa = (0, 1, 0)$ and $\nu = (\nu_i = 0)_{i \in \mathbb{Z}}$. □

3.3 Greene's invariants

We give a geometric description of the soliton lengths of periodic PNG dynamics $\boldsymbol{h}(t)$. For this we introduce up-right paths and simple loops on the cylinder $\mathcal{C}$. An *up-path* ω on $\mathcal{C}$ of length k is a sequence of points $\omega = (p_1, \ldots, p_k) \in \mathcal{C}^k$ such that $p_{i+1} \sim p_i + (\xi, \tau)$ for $(\xi, \tau) \in \mathbb{R}^2$ with $\tau \geq |\xi|$, for $i = 1, \ldots, k-1$. A *simple loop* γ on $\mathcal{C}$ of length k is a sequence of points $((x_1, t_1), \ldots, (x_k, t_k)) \in \mathcal{C}^k$ such that $-\frac{1}{2} < x_1 < \cdots < x_k \leq \frac{1}{2}$ and $(x_{i+1}, t_{i+1}) = (x_i, t_i) + (\xi, \tau)$ with $|\tau| < \xi < 1$ for all $i = 1 \ldots, k$, where $(x_{k+1}, t_{k+1}) = (x_1, t_1)$ by convention. For examples, see Figure 3 (fourth panel).

On point configurations $\boldsymbol{p} \in \mathring{\mathcal{P}}_n$ we define the statistics

$$LPP_k(\boldsymbol{p}) = \max_{\substack{\omega_1, \ldots, \omega_k \\ \text{disjoint} \\ \text{up-paths}}} \left\{ \sum_{i=1}^{k} \ell(\omega_k) \right\} \quad \text{and} \quad LPP_k^{\mathrm{loop}}(\boldsymbol{p}) = \max_{\substack{\gamma_1, \ldots, \gamma_k \\ \text{disjoint} \\ \text{simple loops}}} \left\{ \sum_{i=1}^{k} \ell(\gamma_k) \right\}. \tag{3.1}$$

Theorem 11. *Let $h \in \mathring{\mathcal{S}}$ and let $\boldsymbol{p} \in \mathcal{P}_n$ such that $\Upsilon(h) = (\boldsymbol{p}, \nu)$. Let μ be the shape of (H_1, H_2) corresponding to h under the bijection ψ. Then, we have*

$$LPP_k(\boldsymbol{p}) = \mu_1 + \cdots + \mu_k \qquad \text{and} \qquad LPP_k^{\mathrm{loop}}(\boldsymbol{p}) = \mu'_1 + \cdots + \mu'_k. \tag{3.2}$$

4 Summation identities

An important statistics over the set $\mathrm{HST}(\mu)$ is the energy function E. Its definition is combinatorial can be found in [14]; we use it in the definition of the transformed Hall–Littlewood functions[2] with Plancherel specialization. For a partition μ and $t > 0$, define

$$\mathcal{H}_\mu(t; q) = \sum_{H \in \mathrm{HST}(\mu)} q^{E(H)} t^{|\mu|}. \tag{4.1}$$

[2]The transformed Hall–Littlewood polynomials are related to the modified Macdonald polynomials of [6] as $\mathcal{H}(x; q) = q^{\sum_i (i-1)\lambda_i} \tilde{H}_\lambda(x; 0, q^{-1})$. In particular we set Macdonald's t-parameter to q^{-1} and Macdonald's q-parameter to 0. Here we only consider their Plancherel specialization.

The above construction gives bijective proofs of summation identities for the transformed Hall–Littlewood polynomials $\mathcal{H}$, which are refinements of their Cauchy and Littlewood identities. Similar identities were proven in [10, 7] and in [8, 9] through vertex model techniques. While the summations below can be derived from those of [10] by a change of specialization, their bijective proof is new.

We use the q-Pochhammer symbols $(z;q)_k = \prod_{j=0}^{k-1}(1-zq^j)$ and $(a_1,\dots,a_m;q)_k = \prod_{j=1}^{m}(a_j;q)_k$, for $k \in \mathbb{N}\cup\{\infty\}$. We also use the q-binomial coefficient $\binom{n}{k}_q = \frac{(q;q)_n}{(q;q)_k(q;q)_{n-k}}$.

Theorem 12. *For $|q|<1, \alpha,\beta\in\mathbb{R}$ define*

$$b_\mu(q) = \prod_{i\geq 1}(q;q)^{-1}_{\mu_i'-\mu_{i+1}'} \qquad b_\mu(\alpha,\beta;q) = \prod_{i\ even}\frac{[1+q\alpha\beta]_{q^2}^{m_i(\mu)}}{(q^2;q^2)_{m_i(\mu)}}\prod_{i\ odd}\frac{[\alpha+q\beta]_{q^2}^{m_i(\mu)}}{(q^2;q^2)_{m_i(\mu)}}$$

where $m_i(\mu) = \big|\{j:\mu_j=i\}\big|$ and $[a+b]_p^n = \sum_{k=0}^n \binom{n}{k}_p a^{n-k}b^k$. Then, we have

$$\sum_{\rho\subset\lambda\,:\,\lambda_1'=\ell} q^{|\rho|}s_{\lambda/\rho}(t)^2 = \sum_{k=0}^{\ell}\frac{q^{\ell-k}}{(q;q)_{\ell-k}}\sum_{\mu\,:\,\mu_1'=k} b_\mu(q)\mathcal{H}_\mu(t;q)^2 \tag{4.2}$$

$$\sum_{\rho\subset\lambda\,:\,\lambda_1'=\ell} \alpha^{\mathrm{or}(\lambda)}\beta^{\mathrm{or}(\rho)}q^{|\rho|}s_{\lambda/\rho}(t) = \sum_{k=0}^{\ell}\frac{[q\alpha\beta+q]_{q^2}^{\ell-k}}{(q^2;q^2)_{\ell-k}}\sum_{\mu\,:\,\mu_1'=k} b_\mu(\alpha,\beta;q)\mathcal{H}_\mu(t;q^2), \tag{4.3}$$

where $\mathrm{or}(\lambda)$ *is the number of odd elements of* λ.

5 q-PNG models in full and half space

Similar to (1.1), we introduce the set of height functions

$$\mathsf{PW}_{\mathbb{A}} = \{h\colon \mathbb{A}\to\mathbb{Z} : h(x)-h(x_\pm)\in\{0,1\}\ \forall x \text{ and } |\{x:h(x)\neq h(x_\pm)\}|<\infty\}, \tag{5.1}$$

for $\mathbb{A}\in\{\mathbb{R},\mathbb{R}_+\}$. We also fix $\{B_q(x,t) : x\in\mathbb{R}, t>0\}$ a family of independent and identically distributed Bernoulli random variable of mean q. We assume $q\in(0,1)$.

5.1 The q-deformed polynuclear growth

The q-PNG [1] is a random dynamics of a height $h(\cdot,t)\in\mathsf{PW}_{\mathbb{R}}$, following three rules:

1. **(Lateral propagation)** The up-jumps (resp. down-jumps) of h move with unit speed to their left (resp. to their right).
2. **(Merging of islands)** If a down-jump and an up-jump of h collide at a point x at time t they annihilate with probability $1-q$ and with probability q they generate a nucleation on top of x; i.e., we have $h(y,t) = h(y,t_-) + (1+B_q(x,t))\,\mathbf{1}_{y=x}$.

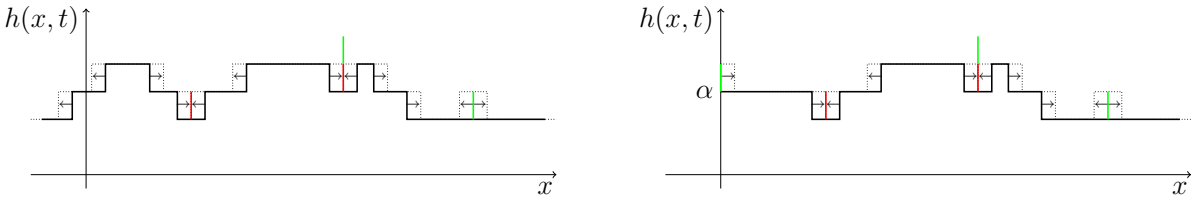

Figure 4: In the left panel, a depiction of the q-PNG dynamics. In the right panel, the q-PNG dynamics in half space. Nucleations at the origin occurr with rate α.

3. **(Poisson random nucleations)** Let $\mathfrak{P} \subset \mathbb{R} \times \mathbb{R}_+$ be a space-time Poisson point process. Then for any $(x,t) \in \mathfrak{P}$ we have $h(y,t) = h(y,t^-) + \mathbf{1}_{y=x}$.

We will consider the *droplet initial condition* at $x \in \mathbb{R}$, which means $h(y,0) = -\infty \mathbf{1}_{y \neq x}$ or the initial height takes value 0 at $y = x$ and $-\infty$ elsewhere.

Theorem 13 ([1]). *Let $h(x,t)$ be the q-PNG height function with droplet initial condition at 0. Then, we have $h(0,t) \sim \mu_1'$, where μ is a partition taken with law $e^{-t^2/(1-q)} b_\mu(q) \mathcal{H}_\mu(t;q)^2$.*

5.2 The q-deformed polynuclear growth in half-space

We introduce the q-deformed polynuclear growth in half-space. It is a stochastic dynamics on height functions $h(\cdot,t) \in \mathsf{PW}_{\mathbb{R}_+}$, which follow rules 1, 2, 3 above and additionally

4. **(Islands hitting the origin)** In case a down-jump collides with the origin at time t, then we set $h(y,t) = h(y,t^-) + (1 + B_q(0,t))\mathbf{1}_{y=0}$.

5. **(Nucleation at the origin)** Let $\mathfrak{O} \subset \mathbb{R}_+$ be a Poisson point process with rate $\alpha > 0$. Then for any $t \in \mathfrak{O}$ we have $h(y,t) = h(y,t_-) + \mathbf{1}_{y=0}$.

The half-space q-PNG can be viewed as a full-space q-PNG with noise and initial data symmetric with respect to the origin and with additional sources of nucleation at the origin. This model has not appeared earlier in literature, although it can be obtained as a scaling limit of the q-pushTASEP with particle creation introduced in [2]. The next theorem follows from a scaling limit of [2, Proposition 4.24].

Theorem 14. *Let $h(x,t)$ be the half space q-PNG height function with droplet initial condition at 0 and nucleation rate α at the origin. Then, we have $h(0,t) \sim \mu_1'$, where μ is a random partition with probability mass function $e^{-(t^2+2\alpha t)/2(1-q)} \mathcal{E}_\mu(\alpha;q) \mathcal{H}_\mu(t;q)$;*

$$\mathcal{E}_\lambda(\alpha;q) = \sum_{\mu' \text{ even}} b_\mu(0,0;q^{1/2}) \varphi_{\lambda/\mu}(q) \alpha^{|\lambda/\mu|}, \quad \varphi_{\lambda/\mu}(q) = \frac{1}{(q;q)_{\lambda_1-\mu_1}} \prod_{i \geq 1} \begin{pmatrix} \mu_i - \mu_{i+1} \\ \mu_i - \lambda_{i+1} \end{pmatrix}_q.$$

5.3 Exact formulas

We now present exact determinantal and Pfaffian formulas that describe the height distribution in the q-PNG in full and half space. Theorem 15 is an immediate consequence of Theorem 13, (4.2) and of the fact that the l.h.s. of (4.2), after a certain shift, can be expressed as Fredholm determinant [4]. Theorem 16 follows from Theorem 14, (4.3), a special symmetry of the half-space q-Whittaker measure [2] and from the fact the fact that the l.h.s. of (4.3), after a certain shift, can be expressed as Fredholm Pfaffian [3]. The results Theorem 16 would yields asymptotics for the half-space q-PNG similar to [11, 7].

Below we say that random variables χ and S have respectively q-geometric and $\mathrm{Theta}(\zeta, q)$ distribution (in short $\chi \sim q\text{-Geo}(q)$ and $S \sim \mathrm{Theta}(\zeta, q)$) if $\mathbb{P}(\chi = k) \propto \frac{q^k}{(q;q)_k}$, for $k \in \mathbb{Z}_{\geq 0}$ and $\mathbb{P}(S = \ell) \propto \zeta^\ell q^{\ell^2}$ for $\ell \in \mathbb{Z}$.

Theorem 15. *Let $h(x,t)$ be the q-PNG height function with droplet initial conditions at the origin and let $\chi \sim q\text{-Geo}(q)$, $S \sim \mathrm{Theta}(\zeta, q)$ be independent random variables. Then, we have*[3]

$$\mathbb{P}\left[h(0,t) + \chi + S \leq s\right] = \det\left[1 - \mathcal{K}^t\right]_{\ell^2\{s+\frac{1}{2}, s+\frac{3}{2}, \dots\}} \qquad \forall s \in \mathbb{Z}, \tag{5.2}$$

$$\text{with kernel } \mathcal{K}^t(a,b) = \oint_{|z|=q^{-1/4}} \oint_{|w|=q^{1/4}} \frac{w^{b-1/2}}{z^{a+3/2}} \frac{e^{\frac{t}{1-q}(z-z^{-1})}}{e^{\frac{t}{1-q}(w-w^{-1})}} \frac{(q, q, \frac{\zeta z}{w}, \frac{qw}{\zeta z}; q)_\infty}{(\frac{w}{z}, \frac{qz}{w}, \zeta, \frac{q}{\zeta}; q)_\infty} \frac{\mathrm{d}z}{2\pi \mathrm{i}} \frac{\mathrm{d}w}{2\pi \mathrm{i}}. \tag{5.3}$$

Theorem 16. *Let $h(x,t)$ be the half-space q-PNG height function with droplet initial condition at the origin and nucleation rate α at the origin. Let $\chi \sim q\text{-Geo}(q)$, $S \sim \mathrm{Theta}(\zeta^2, q^2)$ be independent random variables. Let $M = \min\{\alpha^{-1}, q^{-1/2}\}$. Then, we have*[4]

$$\mathbb{P}\left[h(0,t) + \chi + 2S \leq s\right] = \mathrm{Pf}\left[J - \mathcal{L}^{t,\alpha}\right]_{\ell^2\{s+\frac{1}{2}, s+\frac{3}{2}, \dots\}} \qquad \forall s \in \mathbb{Z} \tag{5.4}$$

$$\text{with kernel } \mathcal{L}^{t,\alpha}(a,b) = \begin{pmatrix} L^{t,\alpha}(a,b) & -2\nabla_b L^{t,\alpha}(a,b) \\ -2\nabla_b L^{t,\alpha}(a,b) & 4\nabla_a \nabla_b L^{t,\alpha}(a,b) + \Delta'(a,b) \end{pmatrix}, \tag{5.5}$$

where $\nabla_a f(a) = \frac{1}{2}\left[f(a+1) - f(a-1)\right]$, $\Delta'(a,b) = \mathbf{1}_{b=a+1} - \mathbf{1}_{b=a-1}$ and, for $r \in (1, M)$,

$$\begin{aligned} L^{t,\alpha}(a,b) = \oint_{|z|=r} \oint_{|w|=r} \frac{w^{b-1/2}}{z^{a+3/2}} e^{\frac{t}{1-q}(z+w-z^{-1}-w^{-1})} \frac{(\frac{\alpha}{z}, \frac{\alpha}{w}; q)_\infty}{(\alpha z, \alpha w; q)_\infty} \\ \times \frac{(q, q, \frac{w}{z}, \frac{qz}{w}; q)_\infty}{(\frac{1}{z^2}, \frac{1}{w^2}, \frac{1}{zw}, qzw; q)_\infty} \frac{(\zeta^2 z^2 w^2, \frac{q^2}{\zeta^2 z^2 w^2}; q^2)_\infty}{(\zeta^2, \frac{q^2}{\zeta^2}; q^2)_\infty} \frac{\mathrm{d}z}{2\pi \mathrm{i}} \frac{\mathrm{d}w}{2\pi \mathrm{i}}. \end{aligned} \tag{5.6}$$

[3] We denote $\det[1 - K]_{\mathcal{L}^2(\Omega,\nu)} = \sum_{k \geq 0} \frac{(-1)^k}{k!} \int_{\Omega^k} \det(K(\xi_i, \xi_j))_{i,j=1}^k \nu(d\xi_1) \cdots \nu(d\xi_k)$ the Fredholm determinant of the kernel K over the Hilbert space $\mathcal{L}^2(\Omega, \nu)$.

[4] We denote $\mathrm{Pf}[J - L]_{\mathcal{L}^2(\Omega,\nu)} = \sum_{k \geq 0} \frac{(-1)^k}{k!} \int_{\Omega^k} \mathrm{Pf}(L(\xi_i, \xi_j))_{i,j=1}^k \nu(d\xi_1) \cdots \nu(d\xi_k)$ the Fredholm Pfaffian of the 2×2-matrix valued skew-symmetric kernel L over the Hilbert space $\mathcal{L}^2(\Omega, \nu)$.

References

[1] A. Aggarwal, A. Borodin, and M. Wheeler. "Deformed Polynuclear Growth in (1+1) Dimensions". *Int. Math. Res. Not.* **2023**.7 (Mar. 2023), pp. 5728–5780. DOI.

[2] G. Barraquand, A. Borodin, and I. Corwin. "Half-Space Macdonald Processes". *Forum Math., Pi* **8** (2020), e11. DOI.

[3] D. Betea, J. Bouttier, P. Nejjar, and M. Vuletić. "The Free Boundary Schur Process and Applications I". *Annales Henri Poincaré* **19** (12 Dec. 2018), pp. 3663–3742. DOI.

[4] A. Borodin. "Periodic Schur process and cylindric partitions". *Duke Math. J.* **140**.3 (2007), pp. 391–468. DOI.

[5] D. Bump and A. Schilling. *Crystal Bases*. World Scientific, 2017. DOI.

[6] J. Haglund, M. Haiman, and N. Loehr. "A combinatorial formula for Macdonald polynomials". *J. Amer. Math. Soc.* **18**.3 (2005), pp. 735–761. DOI.

[7] J. He. "Boundary current fluctuations for the half space ASEP and six vertex model". *Proc. London Math. Soc.* **128** (2024), e12585. DOI.

[8] J. He and M. Wheeler. "Periodic q-Whittaker and Hall–Littlewood processes". *Selecta Mathematica* **32**.1 (2026), p. 11. DOI.

[9] J. He and M. Wheeler. "Symmetries of periodic and free boundary q-Whittaker measures". *Sem. Loth. Combin.* **93B** (2025), #133.

[10] T. Imamura, M. Mucciconi, and T. Sasamoto. "Skew RSK dynamics: Greene invariants, affine crystals and applications to q-Whittaker polynomials". *Forum Math. Pi* **11**.e27 (2023), pp. 1–101. DOI.

[11] T. Imamura, M. Mucciconi, and T. Sasamoto. "Solvable models in the KPZ class: Approach through periodic and free boundary Schur measures". *Ann. Probab.* **54**.1 (2026), pp. 301–366. DOI.

[12] T. Imamura, M. Mucciconi, T. Sasamoto, and T. Scrimshaw. "Skew Column RSK dynamics and the Box and Ball System". In preparation.

[13] R. Inoue, A. Kuniba, and T. Takagi. "Integrable structure of box–ball systems: crystal, Bethe ansatz, ultradiscretization and tropical geometry". *Journal of Physics A: Mathematical and Theoretical* **45**.7 (2012), p. 073001. DOI.

[14] A Nakayashiki and Y. Yamada. "Kostka polynomials and energy functions in solvable lattice models". *Selecta Math.* **3** (4 1997), pp. 547–599. DOI.

[15] M. Prähofer and H. Spohn. "Scale invariance of the PNG droplet and the Airy process". *J. Stat. Phys.* **108** (2002). arXiv:math.PR/0105240, pp. 1071–1106. DOI.

[16] B. Sagan and R. Stanley. "Robinson–Schensted algorithms for skew tableaux". *J. Combin. Theory Ser. A* **55**.2 (1990), pp. 161–193. DOI.

[17] D. Takahashi and J. Satsuma. "A soliton cellular automaton". *J. Phys. Soc. Japan* **59**.10 (1990), pp. 3514–3519. DOI.